Journal of the American Mosquito Control Association, 39(4):223–230, 2023

UNCREWED AERIAL SPRAY SYSTEMS FOR MOSQUITO CONTROL: EFFICACY STUDIES FOR SPACE SPRAYS

JANE A. S. BONDS,[1] BRAD K. FRITZ,[2] HAROLD THISTLE,[3] MIRANDA TRESSLER,[4] SARAH S. WHEELER,[5] REBECCA HARSHAW,[4] BILL REYNOLDS[6] AND PIPER KIMBELL[6]

ABSTRACT. Achieving an appropriate droplet size distribution for adulticiding has proved problematic for unmanned aerial spray systems (UASSs). The high-pressure pumping systems utilized on crewed aircraft conflict with the weight constraints of UASSs. The alternative is a lightweight rotary atomizer, which when run at a maximum rpm with a minimal flow rate can achieve the appropriate droplet size distribution. For this study a UASS was calibrated to discharge an appropriate droplet size distribution ($Dv_{0.5}$ of 48 μm and $Dv_{0.9}$ of 76 μm). Spray was released from an altitude of 23 m (75 ft). The spray plume was shown to effectively disperse through the sampling zone. To achieve the appropriate application rate, the flight speed was 3 m/sec (6.7 mph) with an assumed swath of 150 m (500 ft). The objective of this project was not to conduct an operational application; instead only 1 flight line was used so that the effective swath width could be confirmed and the appropriate flightline separation defined. This study showed that control was achieved across distances of 100–150 m. Considering a swath width of 150 m (500 ft), ground deposition was 13–36% of applied material. Spray deposition corresponded well with the mortality data, which helped improve confidence in the data. The overall conclusion from this study is that aerial adulticiding is feasible with the system presented here. Further work is required to improve the atomization system to allow operational flight speeds and to determine the interaction between release altitude and droplet size in order to minimize ground deposition of application material.

KEY WORDS Efficacy studies, mosquito adulticide, space spray, system, system optimization, unmanned aerial spray

INTRODUCTION

For many years mosquito control programs have utilized conventional aircraft for wide-area applications of both adulticides and larvicides (Bonds 2012, Mount 1985, Likos et al. 2016). However, because of their size and speed, crewed aircraft require large areas to operate, and the low-altitude maneuvers required by many mosquito management applications make applications difficult, especially in densely populated areas and congested airspace. Often mosquito control applications are required in areas with obstacles such as power lines and cell phone towers that are problematic for crewed aircraft. Unmanned aircraft, however, fly at low altitudes and slow speeds and can be equipped with obstacle detection sensors that prevent collisions and permit autonomous maneuvers around obstacles (Williams et al. 2020).

The Department of Defense explored the use of the RMAX (Yamaha Motor Company, Iwata, Shizuoka, Japan) for mosquito control spraying to protect soldiers overseas from biting insects (Miller 2005). Unfortunately, the RMAX was expensive ($86,000 to $1,000,000 depending on configuration) and required extensive training to fly (Hanlon 2004). Those factors, combined with prohibitive regulations and technical difficulties, caused the military to transfer the project to the US Department of Agriculture in 2004 (Cope et al. 2008). Researchers made significant improvements to the application technologies (Huang et al. 2009, 2013), but unmanned aircraft systems (UASs) remained too expensive and difficult to fly to be practical for mosquito management.

Over the years, the costs associated with these vehicles have reduced significantly. A small fleet of unmanned aerial spray systems (UASSs) would cost the equivalent of 1 day of contracted aerial application service, making aerial applications available to any size mosquito control program in any type of environment (Faraji et al. 2021). More confidence in the ability of UASSs to operate safely and effectively is needed, however, for regulators to develop guidelines for use. For instance, the Environmental Protection Agency pesticide regulations will require modification to include UASSs. In addition, the requirements of a pesticide label, which dictate the directions of its use, will need to be amended to include UASS application guidelines. Data on both the efficacy of a compound and the methods used to apply it are requirements for public health pesticides. Data are also needed for the protection of nontargets. The exposure of nontargets in adulticide applications is measured as ground deposition. In addition, pesticide drift data are needed for UASSs to minimize the risk of pesticides drifting to nontarget areas (Petty and Chang 2018).

Adulticide applications for mosquito control are typically ultra-low-volume (ULV) aerosol applications, also called space sprays. Droplets drift through the

[1] Bonds Consulting Group, 3900 Wasp Street, Panama City Beach, FL 32408.
[2] Aerial Application Technology Research, USDA ARS, 3103 F&B Road, College Station, TX 77845.
[3] TEALS, LLC, 775 State Route 248, Whitesville, NY 14897.
[4] Volusia County Mosquito Control, 801 South Street, New Smyrna Beach, FL 32168.
[5] Sacramento-Yolo Mosquito and Vector Control District, 8631 Bond Road, Elk Grove, CA 95624.
[6] Leading Edge Associates, 1425 Tomoka Farms Road, Daytona Beach, FL 32124.

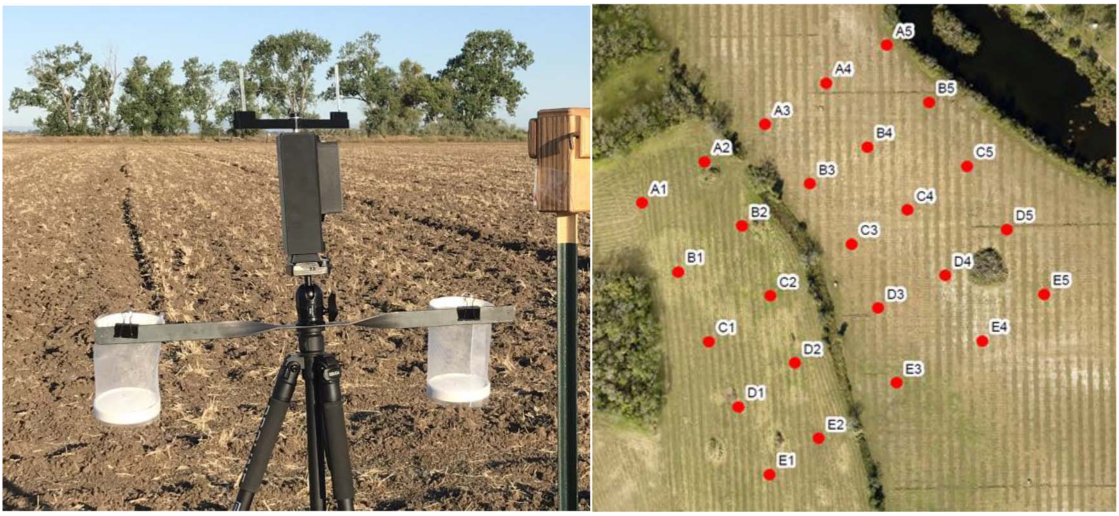

Fig. 1. Bioassay cages and rotating impactor with the deposition sampler on the ground out of the picture (left) and the field site with the samples stations marked (right).

target area and impact flying mosquitoes. Adulticide applications apply concentrate formulated pesticide; during this study the application rate was 73 ml/ha (1 oz/acre). The ULV applications lend themselves to the weight constraints of UASS because the low volumes applied result in payloads well within the capacity of UASSs.

Previous physical characterization studies (Bonds et al. unpublished data) investigated spray deposition downwind of UASS adulticide applications to identify an appropriate flight line separation for a uniform distribution of the spray cloud. These studies showed that the spray began to descend in the first 50 m (160 ft) across a 150 m (500 ft) swath. This is approximately half the flight line separation for manned aircraft (300 m), which is understandable because the droplet size distribution and flight altitude are slightly larger and lower, respectively, than with manned aircraft. The language on most labels states that the median droplet size is $Dv_{0.5} < 60$ µm and $Dv_{0.9} < 100$ µm. The typical minimum release height on an adulticide label would be > 30 m (100 ft). With typical ULV applications, the majority of the spray cloud should remain airborne with minimal deposition. Concerns over human and environmental exposure due to ground deposition must be addressed, so this study presents both the effective swath measured via caged mosquito bioassays and nontarget effects measured via ground deposition samplers.

MATERIALS AND METHODS

Treatments: The UASS was set up to release a droplet size of $Dv_{0.5}$ 48 µm and a $Dv_{0.9}$ 76 µm from an altitude of 23 m (75 ft) over a range of meteorological conditions. Each flight line was chosen prior to application to be perpendicular to the predominant wind direction with 1 pass on the downwind edge of the sample matrix. The flightline was approximately 600 m, 3 times the length of the sample grid. There was a total of 6 successful replicates. The first trial operated at a lower altitude than intended so is not presented here.

Previous studies showed that depending on the ambient wind speed, much of the spray cloud descends within 150 m of the flight line. With that knowledge the sampling stations were arranged in a 200 × 200 m (600 ft) matrix with 50 m (160 ft) of separation between each station (Fig. 1). Each application was assessed using Mylar (10 × 10 cm) cards positioned on top of the vegetation for ground deposition measures. Each card was collected in a prelabeled zip top plastic bag and returned to the laboratory for sample processing and analysis. Mortality measures were taken with cylindrical bioassay cages (Fig. 1). Cages were constructed following the design described by the Manatee County Mosquito Control District (Williams 2018). Foam board was substituted with paper ice cream cup lids to reduce extensive labor time needed to cut foam pieces. Each bioassay cage contained approximately 20 female, non-blood-fed, susceptible strain *Culex quinquefasciatus* Say (Benzon Research Carlisle, PA). Exposed cages were returned to the laboratory, and mortality rates were read 24 h postexposure.

The UASS platform used in these studies was the PrecisionVision 35 (Leading Edge Associates, Daytona Beach, FL), which consists of the airframe, propulsion, navigation, and spraying systems. The aircraft operated at 3 m/sec at an altitude of 23 m (75 ft). The active ingredient (AI) was Imperium (Envu Environmental Science NC) with the fluorescent tracer Uvitex OB (2,5-thiophenediylbis[5-tert-butyl-1,3-benzoxazole]; BASF, Florham Park, NJ) added at a rate of 2 g/liter. Spray solutions were mixed in a 20-liter batch, ensuring the

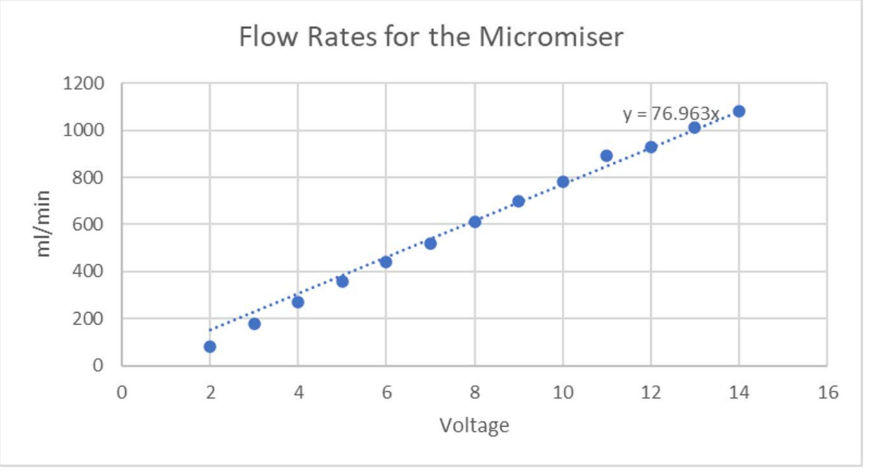

Fig. 2. Flow rates from the 2 Micromiser nozzles for each measured voltage.

dye was completely and uniformly mixed prior to adding to the tank of the UAV. The amount of spray solution in the tank was measured at the beginning and end of each treatment to provide an exact amount applied. It is extremely important to do this to ensure that the correct amount was applied and that there was no application failure. The parameters were the following:

- Flight time range: 13–16 min
- Payload capacity: 10–16 kg
- Payload volume capacity: 16 liters
- Batteries: 2 × 24 V
- Recharge time: 45 min at 30% charge
- Max weight: 24.9 kg for FAA Part 107
- Max speed: 13.4 m/sec
- Hover time: 20 min no payload, 13 min with 10 kg of payload
- Max climb speed: 5 m/sec
- Max descent speed: 3 m/sec

PV-35 Dimensions:

- 6 rotor (hexacopter), 2 Micromiser
- Individual rotor diam 77.47 cm
- Rotor tip to nozzle vertically 45.7 cm
- Nozzle approximately 4 cm in-board from rotor tip
- 241 cm rotor tip to rotor tip (total diam)
- 238.7 cm nozzle body center to nozzle body center
- Tank shape 35.5 × 50.8 cm in horizontal plane
- 39.7 cm from drone top to tank bottom

Micromiser calibration: The test compound was atomized via a rotating disc nozzle called a Micromiser 16 (Micron Group, Bromyard, UK). Two Micromiser atomizers were configured 2.5 m apart on a carbon fiber boom mounted to the landing gear of the drone. The Micromiser has a maximum rotational speed of 16,000 rpm fed by a separate battery and running at full capacity (24 V). The pump speed and therefore flow rate were controlled remotely by changing input voltage from a 24 V battery supply to a voltage between 7 and 18 V (Fig. 2), depending on the droplet size required; as the flow is reduced, so is the droplet size (Table 1).

Droplet sizing: Droplet sizing was conducted at the USDA-ARS-Aerial Application Technology Research Unit's aerial nozzle testing facility in College Station, TX. The Micromiser nozzle was electrically wired to the UAV spray and control system with the plane of rotation oriented perpendicular to laser line of measurement. Droplet-size measurements were made using laser diffraction (Sympatec HELOS, Clausthal-Zellerfeld, Germany). All testing was conducted with the manufacturer-denoted R5 lens (dynamic size range of 0.5/4.5–875 μm across 31 bins). The nozzle was positioned 30 cm upstream of the measurement zone. Each replicated measurement consisted of the nozzle operating for approximately 5 sec. A minimum of 3 replicated measurements were made to ensure that standard deviations were within 10% of the means for each volume diameter recorded. The $DV_{0.1}$, $DV_{0.5}$, and $DV_{0.9}$ (droplet diameter such that 10%, 50%, or 90% of the total spray volume comprised droplets of lesser diameter) were then calculated (ASABE 2012).

The lowest flow rate (154 ml/min, 2 nozzles; Table 1) that returned a droplet size distribution with a $Dv_{0.5}$ of 48 μm at a forward speed of 3 m/sec (7 mph) was used to achieve an application rate of 1.5 g AI/ha (0.00134 lb ai/ac) with an assumed

Table 1. Voltage for the rotation was maintained at full speed 16,000 rpm; adjustments to the pump voltage change the flow rate and therefore droplet size distribution.

Pump voltage (V)	$Dv_{0.1}$	$Dv_{0.5}$	$Dv_{0.9}$	Flow rate (ml/min)
6.29	36	88	134	462
4	32	73	115	308
3	28	65	102	231
2	23	48	76	154

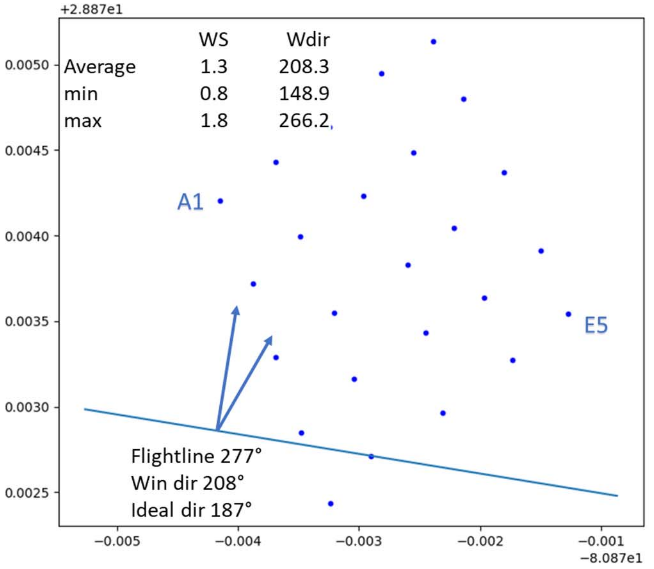

Percent mortality

	1	2	3	4	5
A	19	19	90	100	83
B	8	100	88	100	94
C	100	100	64	100	100
D	0	40	100	100	100
E	0	0	100	85	100

Deposition % applied

	1	2	3	4	5
A	2	17	66	30	64
B	9	36	4	7	163
C	132	171	24	21	6
D	4	7	15	25	15
E	0	22	32	30	0

Fig. 3. Replicate 2: Started with 1.08 m/sec from the SSW with only slight changes in wind direction and speed.

swath of 100 m (330 ft). This flight speed is likely too slow to be operationally relevant, but a faster forward speed required a higher flow rate that resulted in an increased droplet size. During this study achieving an appropriate droplet size distribution took precedence over logistics.

Sample processing and data analysis: Tank samples were collected after each treatment for volumetric analysis via fluorescent spectroscopy in the laboratory (Fritz et al. 2011). The collected tank samples were used to generate a set of reference standard concentrations ranging from 2 to 0.001 ppm. Within these ranges, there was a linear relationship between dye concentration and fluorescent response, allowing for direct calculation of dye concentration in a sample of interest based on its fluorescent reading.

All exposed samples deployed for deposition analysis were collected into prelabeled zip-top bags for processing. Mylar card samples were washed in hexane with a wash volume of 10 ml. Each sample was agitated by hand to ensure complete recovery of dye into wash volume. After washing, 5 ml of analyte was decanted into a glass cuvette that was capped and placed into a prelabeled vial rack. All vialed samples were analyzed for fluorescent emission using a fluorometer with an excitation frequency of 408 nm (Trilogy Fluorometer; Turner Designs San Jose CA).

Meteorological measurements: The meteorological tower was set up and remained in place for the duration of the study. The study was conducted on property that belonged to Volusia County, Florida. To accommodate the study, county employees removed the majority of the vegetation to create a semi-open field for the trial. There were still some trees running through the center of the sampling matrix that could have created an interruption of the air flow adding to the variability in spray distributions (Fig. 1).

The meteorological tower was situated 10 m north of sample Station A3 (28.873782°–80.872730°). The tower consisted of a cup anemometer and wind vane (Model 034B, Met One Instruments, Grants Pass, OR) with 0.1 ms^{-1} accuracy, 0.22 ms^{-1} stall velocity, ± 4° directional accuracy, and 0.4 ms^{-1} vane stall velocity, which were used in real time to determine the flight line based on wind conditions at the time of take-off. The tower also included relative humidity (RH), temperature (T), and solar radiation (QR). The instruments were mounted at a 2.1 m height [RH/T Model 085-35; Met One Instruments; RH 3% accuracy) and the QR sensor (Model 094-1; Met One Instruments; QR ± 3% accuracy)].

RESULTS

The first step in the analysis process was to calculate how far each sample station was from the flightline for each treatment. The approach taken was to calculate the perpendicular distance between the station point and flight line, and the distance along the direction of the mean wind direction. Neither approach resulted in a clear response of mortality or deposition with distance. Throughout these adulticiding studies, wind speed and direction were light and variable, and the treatment period spanned over 30–40 min depending on the wind speed at time of application. Thus, the spray cloud was not necessarily moving in one consistent direction. The position of the flightline relative to the sampling grid (grid axes equals location in decimal degrees) is provided along with the average minimum and maximum wind speeds and direction in degrees (Figs. 3–8).

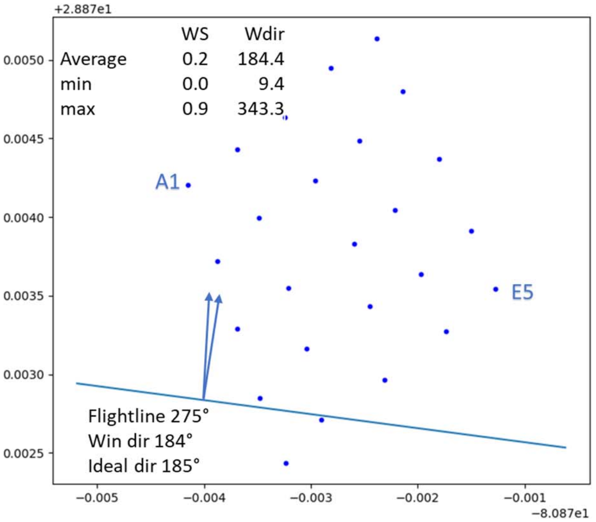

Percent mortality

	1	2	3	4	5
A	59	100	87	81	86
B	100	91	88	82	37
C	100	100	100	100	83
D	80	100	100	100	100
E	0	0	100	100	100

Deposition % applied

	1	2	3	4	5
A	80	41	6	3	3
B	33	6	3	3	5
C	46	29	6	5	11
D	42	150	11	26	9
E	6	16	68	55	8

Fig. 4. Replicate 3: Started at 0 m/sec SE winds, then picked up around halfway with a more southerly direction, dropping off to 0 m/sec again and shifting between E and W.

It can be noted that many of the replicates had wind speeds of 0, the stall speed with these anemometers is 0.4 m/s, and thus, at velocities of less than 0.4 m/s, false readings of 0.0 m/s were collected. When the results were presented graphically the mortality and volumetric data showed complementary trends across the sampling grid. Each replicate therefore was treated as an individual case study. The effective swath from the mortality data spanned across 3 sample stations, which had 50 m separation. The effective spray swath was determined to be 150 m (500 ft); this number was then used for a more accurate application rate measure and subsequent percent of applied calculations. Both mortality and deposition data are presented as percentages. The average deposition ranged from 13% to 36% of applied with a few peaks exceeding 100% of applied.

The flight line for replicate 2 (Fig. 3) was upwind from sample station E1 and directly over the top of D1 and E2. The deposition peak at B5 is noteworthy, because deposition peaks are usually seen near field as the larger droplets deposit closer to the flight line.

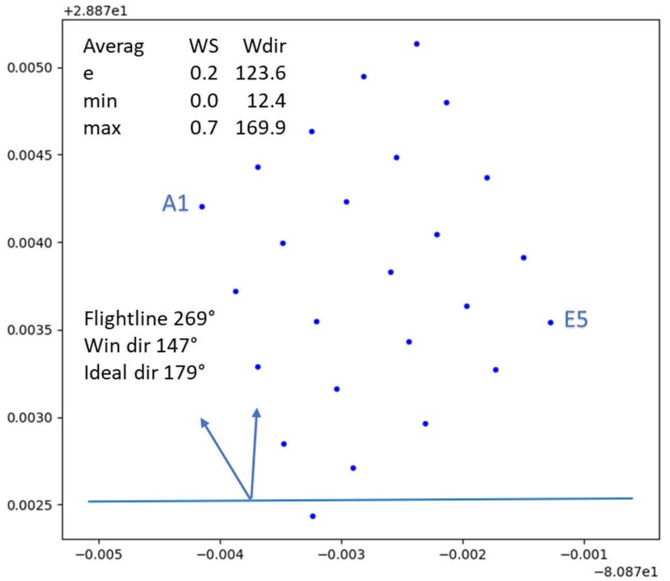

Percent mortality

	1	2	3	4	5
A	0	45	69	100	92
B	23	90	35	80	100
C	100	60	85	100	91
D	4	80	100	83	100
E	0	6	70	90	64

Deposition % applied

	1	2	3	4	5
A	0	69	5	14	7
B	7	39	25	59	8
C	68	38	58	23	8
D	-1	30	122	39	23
E	3	36	12	4	18

Fig. 5. Replicate 4: Started at 0.7 m/sec SE with the speed dropping off to 0 and the direction variable but shifting to the N.

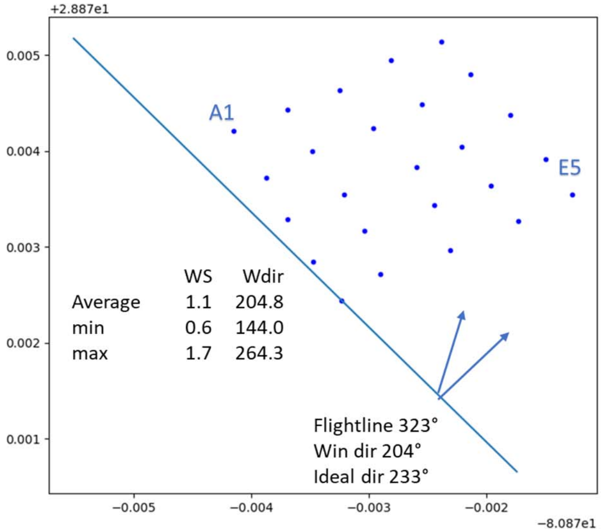

Percent mortality

	1	2	3	4	5
A	100	100	88	100	79
B	95	100	100	100	83
C	93	92	79	100	50
D	0	97	100	88	100
E	0	100	93	60	100

Deposition % applied

	1	2	3	4	5
A	57	6	15	0	5
B	117	31	67	4	3
C	69	29	98	2	1
D	2	54	7	2	14
E	10	50	7	6	5

Fig. 6. Replicate 5: Started at 0.6 m/sec from the S with the speed increasing and the direction shifting to the SW.

The flight line for replicate 3 (Fig. 4) was the same as in replicate 2, but the wind speed was much lower and wind direction was almost perpendicular to the fight line. The mortality data show good control across most of the sample matrix and a deposition peak as expected approximately 50 m from the flightline. The low wind speed led to a near-field deposition maximum, while the descending droplet cloud provided near-complete control across the 200 m matrix, excluding E1 and E2 that were upwind.

The flightline for replicate 4 (Fig. 5) was set based on a S wind direction, but the wind direction flipped to the SE and then N after the start of the application. Mortality was highest on the east side of the sample matrix, which was unexpected based on wind direction. However, it is important to note that the application altitude was 23 m (75 ft) and the weather station was set at 2 m. During the application the wind dropped to zero with cloudy skies; thus, there was a possibility for inversion conditions, so the wind direction at height could have been different than at ground level. Control was still observed despite the shifting wind, the effective swath was 100–150 m, and near-field deposition peaked at 50 m.

For replicate 5 (Fig. 6) a wind from the SW was anticipated, but during the application it shifted to the

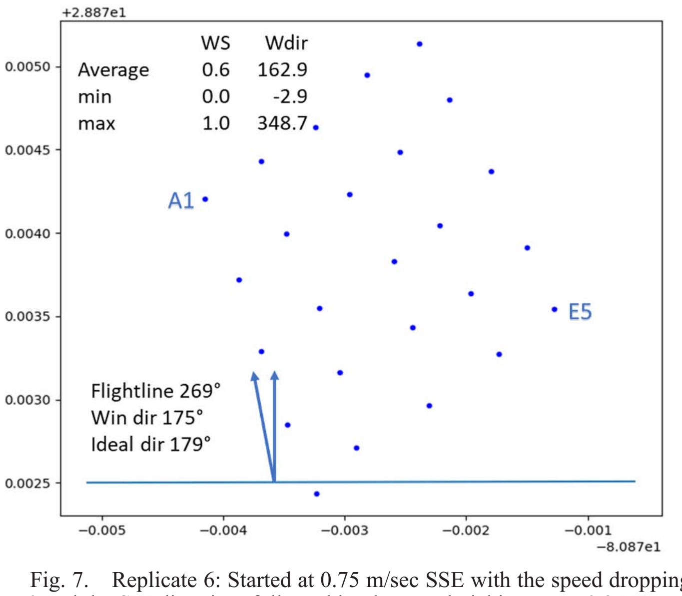

Percent mortality

	1	2	3	4	5
A	100	0	100	100	93
B	100	100	100	100	95
C	100	100	100	100	100
D	50	79	100	100	86
E	0	27	100	100	100

Deposition % applied

	1	2	3	4	5
A	44	15	10	7	10
B	33	10	12	7	10
C	32	27	10	14	8
D	7	29	16	15	16
E	7	23	58	43	10

Fig. 7. Replicate 6: Started at 0.75 m/sec SSE with the speed dropping off shifting to the SE, then the speed dropping to 0 and the SW direction, followed by the speed picking up to 0.3 NE and then 0.6 N.

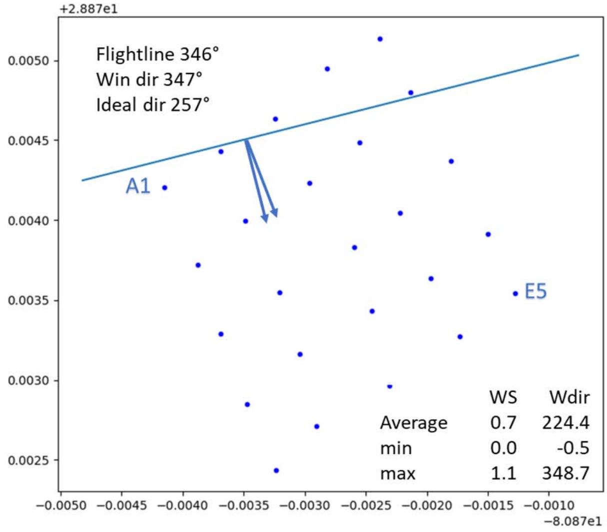

Percent mortality

	1	2	3	4	5
A	67	62	0	100	0
B	13	100	100	100	0
C	4	89	100	100	100
D	0	95	94	100	100
E	5	0	100	0	100

Deposition % applied

	1	2	3	4	5
A	47	6	6	6	6
B	9	22	42	8	6
C	6	12	25	23	21
D	6	7	9	9	15
E	7	6	8	8	12

Fig. 8. Replicate 7: Started at 1.1 m/sec NNW slowing and shifting to the north and wavering back and forth.

S and then back to the SW. The flight line was over station D1 and E1 showing 0 mortality at these stations and low deposition. The deposition peaks were not perfectly aligned with mortality data. In each case deposition was consistently higher closer to the flight line or at the beginning of the effective swath. This is because the larger drops that constitute the majority of the ground deposition deposited closer to the release line than the smaller drops that are more likely to stay aloft to contact flying mosquitoes.

The flight line for replicate 6 (Fig. 7) was set for a NNE wind direction, but the wind shifted to SSE and then back to the N. The deposition and mortality data sit in line with the initial wind direction. This seems to be true for all the replicates apart from replicate 4. Like previous replicates, deposition peaked at 50 m.

During replicate 7 (Fig. 8) the deposition and mortality results were congruent with the prevailing wind direction. Note that replicates 6 and 7 both have rather low deposition numbers. The higher deposition numbers with previous replicates may have been influenced by the tree line bisecting the grid. The presence of elevated vegetation can create friction that causes the wind to trip or roll and may have contributed to deposition peaks.

DISCUSSION

Rotary atomizers have been utilized in conventional mosquito control for many years because they offer an advantage over hydraulic nozzles in producing aerosol droplets when affixed to slow-flying aircraft. The speed of rotation of these atomizers, however, must be high (7,000 rpm or more) and flow rates of insecticides low (2 liters per minute or less per atomizer) to produce aerosol droplets (Mount 1985). For UASSs the advantage of rotary atomizers is the lower weight of the system. In hydraulic atomization the weight of the required pumps reduces the chemical payload capacity. With rotary atomizers the liquid can be fed under low pressure; even a low hydrostatic pressure can suffice. The liquid to be atomized emerges from the feeding nozzle at low speed and minimum pressure difference. The disc rotates, and due to centrifugal acceleration, a liquid film forms. This film becomes thinner with increasing distance from the center release point. Then the saw-tooth edge of the disc forms uniform diameter ligaments that return a narrow droplet size spectrum compared to hydraulic nozzles. With hydraulic nozzles the atomization process begins with a wavy sheet that produces ligaments with many different diameters resulting in a much broader droplet size distribution (Matthews 1998). Within this project we utilized a rotating disc technology (16,000 rpm) that produced a very narrow droplet size distribution ($DV_{0.5}$ of 48 µm and a lower $DV_{0.9}$ 76 µm) compared to conventional hydraulic nozzles.

This study showed that this droplet size distribution produced an effective space spray. When the UASS operated at 23 m (75 ft) the flight line separation would be approximately 150 m to maintain control within a target zone. However, improvements are required to reduce the deposition profiles and to improve the working efficiency of the application settings. Deposition numbers across the sample area averaged between 13% and 36% of applied, which is similar to what is typically seen with manned aerial adulticiding (Mickle et al. 2005). For crewed aerial applications, spray equipment must be adjusted so that the volume median diam produced is less than 60 um ($Dv_{0.5} < 60$ um) and that 90% of the spray is contained in droplets smaller than 100 um ($Dv_{0.9} <$ 100 um). Deposition rates for truck-mounted space sprayers usually have much lower deposition rates due to their smaller droplet size distribution. Most labels state that the volume median diameter is less than 30 um ($Dv_{0.5} < 30$ μm) and that 90% of the spray is contained in droplets smaller than 50 um ($Dv_{0.9} < 50$ μm). Tietze et al. (1994) measured ground deposition with malathion returning an average deposition rate of 5.8%. Ground equipment applies much smaller droplet size distributions because the spray is being released into the target zone so only lateral movement is required. Aerial applications require a certain droplet mass to enable the spray droplets to descend into the target area. The small size of UASSs could enable them to safely fly lower through the target zone, but a smaller droplet size distribution would be required.

To increase the working efficiency of the operation, higher volume flow rates are required. Higher flow rates would lead to an increased droplet size distribution. Droplet size can be maintained with increased flow by increasing the rpm of the atomizer; however, the current rpm of 16,000 rpm is at the upper limit of manufacturer specifications. Another option is to increase the diameter of a rotary atomizer, and the manufacturers of the rotating disc have produced a new nozzle for beta testing this year. There is a limit, however, to how much the diameter can be increased because the mechanical load could become too high, depending on the speed. Future testing will reveal whether the new nozzle design reliably produces the required droplet size at the required flow rate. Another potential option for use on UASSs is to fit several atomizers that when combined deliver the target application rate at a lower flow rate; the additional hardware will reduce the carrying capacity of the aircraft, another logistical barrier that would require further work. Lastly, deposition can be reduced by increasing the altitude of the UASS; all of these options are to be considered in future studies.

ACKNOWLEDGMENTS

This study was sponsored by the Department of the Army, U.S. Army Contracting Command, Aberdeen Proving Ground, Edgewood Contracting Division, Ft Detrick, MD, under Deployed Warfighter Protection (DWFP) Program Grant W911QY1910008 for the research project, characterization of the spray distribution of Remotely-Piloted Aerial Spray Systems (RASS), and development of turnkey systems for vector control. We appreciate the assistance of the following persons with rearing mosquitoes and conducting field operations in Florida: Savannah Stura, May Pivarnik, Grace Hunter, and all supporting staff at Volusia County Mosquito Control. From the California team we thank Debbie Dritz, Kara Kelley, Steve Ramos, Samer Elkashef, Gary Goodman, and the supporting staff at the Sacramento-Yolo Mosquito and Vector Control District.

REFERENCES CITED

ASABE [American Society of Agricultural and Biological Engineers]. 2012. ASABE S327.4. *Terminology and definitions for application of crop or forestry production and protection agents*. St. Joseph, MI: ASABE.

Bonds JAS. 2012. Ultra-low-volume space sprays in mosquito control: a critical review. *Med Vet Entomol* 26:121–130.

Cope SE, Strickman DA, White GB. 2008. The Deployed Warfighter Protection Research Program: finding new methods to vanquish old foes. *US Army Medical Dept J* April to June:9–21.

Faraji A, Haas-Stapleton E, Sorensen B, Scholl M, Goodman G, Buettner J, Schon S, Lefkow N, Lewis C, Fritz B. 2021. Toys or tools? Utilization of unmanned aerial systems in mosquito and vector control programs. *J Econ Entomol* 114:1896–1909.

Fritz BK, Hoffmann WC, Jank P. 2011. A fluorescent tracer method for evaluating spray transport and fate of field and laboratory spray applications. *J Am Soc Trop Med Intl* 8:1–9.

Hanlon M. 2004. Yamaha's RMAX—the world's most advanced non-military UAV. *New Atlas* [Internet] 19:5 [Accessed October 15, 2023]. Available from: https://newatlas.com/yamahas-rmax-the-worlds-most-advanced-non-military-uav/2440/.

Huang Y, Hoffmann WC, Lan Y, Wu W, Fritz BK. 2009. Development of a spray system for an unmanned aerial vehicle platform *Appl Eng Agric* 25:803–809.

Huang Y, Thomson SJ, Hoffmann WC, Lan Y, Fritz BK. 2013. Development and prospect of unmanned aerial vehicle technologies for agricultural production management. *Intl J Agric Biol Eng* 6:1–10.

Likos A, Griffin I, Bingham A, Stanek D, Fischer M, White S, Hamilton J, Eisenstein L, Atrubin D, Mulay P. 2016. Local mosquito-borne transmission of Zika virus—Miami-Dade and Broward Counties, Florida, June–August 2016. *Morb Mort Weekly Report* 65:1032–1038.

Matthews GA. 1998. Application techniques for agrochemicals. In: Matthews GA, Hislop EC, eds. *Chemistry and technology of agrochemical formulations*. Dordrecht, the Netherlands: Springer Netherlands. p. 302–336.

Mickle RE, O. Samuel L, St. Laurent P, Rousseau D, Rousseau G. 2005. Direct comparison of deposit from aerial and ground ULV applications of malathion with AGDISP predictions. In: *REMSpC report* edited by *Institut national de santé publique du Québec*.

Miller JW. 2005. Report on the development and operation of a UAV for an experiment on unmanned application of pesticides. In: *AFRL USAF.*

Mount G. 1985. Ultra-low volume application of insecticides for vector control. In: Division of Vector and Control, ed. *World Health Organization*. Geneva, Switzerland: World Health Organization, WHO/VBC/85.919.

Petty RV, Chang EBE. 2018. Drone use in aerial pesticide application faces outdated regulatory hurdles. *Harvard J Law Tech Dig.* January 16.

Tietze NS, Hester PG, Shaffer KR. 1994. Mass recovery of malathion in simulated open field mosquito adulticide tests. *Arch Environ Contam Toxicol* 26:473–477.

Williams GM, Wang Y, Suman DS, Unlu I, Gaugler R. 2020. The development of autonomous unmanned aircraft systems for mosquito control. *PLoS ONE* 15:e0235548.

Williams K. 2018. A Behind the Scenes Look at caged mosquito field trials performed by Manatee County Mosquito Control District. *Wing Beats* 11–20.